Constitutively Activated STAT3 Frequently Coexpresses with Epidermal Growth Factor Receptor in High-Grade Gliomas and Targeting STAT3 Sensitizes Them to Iressa and Alkylators

Hui-Wen Lo, Xinyu Cao, Hu Zhu, and Francis Ali-Osman

Abstract

Purpose: The goals of this study are to elucidate the relationship of the oncogenic transcription factor signal transducer and activator of transcription 3 (STAT3) with glioma aggressiveness and to understand the role of high STAT3 activity in the resistance of malignant gliomas and medulloblastomas to chemotherapy.

Experimental Design: Immunohistochemical staining and biochemical methods were used to examine the extent of STAT3 activation and EGFR expression in primary specimens and cell lines, respectively. Cellular response to drug treatments was determined using cell cytotoxicity and clonogenic growth assays.

Results: We found STAT3 to be constitutively activated in 60% of primary high-grade/malignant gliomas and the extent of activation correlated positively with glioma grade. High levels of activated/phosphorylated STAT3 were also present in cultured human malignant glioma and medulloblastoma cells. Three STAT3-activating kinases, Janus-activated kinase 2 (JAK2), EGFR, and EGFRvIII, contributed to STAT3 activation. An inhibitor to JAK2/STAT3, JSI-124, significantly reduced expression of STAT3 target genes, suppressed cancer cell growth, and induced apoptosis. Furthermore, we found that STAT3 constitutive activation coexisted with EGFR expression in 27.2% of primary high-grade/malignant gliomas and such coexpression correlated positively with glioma grade. Combination of an anti-EGFR agent Iressa and a JAK2/STAT3 inhibitor synergistically suppressed STAT3 activation and potently killed glioblastoma cell lines that expressed EGFR or EGFRvIII. JSI-124 also sensitized malignant glioma and medulloblastoma cells to temozolomide, 1,3-bis(2-chloroethyl)-1-nitrosourea, and cisplatin in which a synergism existed between JSI-124 and cisplatin.

Conclusion: STAT3 constitutive activation, alone and in concurrence with EGFR expression, plays an important role in high-grade/malignant gliomas and targeting STAT3/JAK2 sensitizes these tumors to anti-EGFR and alkylating agents.

Malignant gliomas are the most common brain tumors in adults (1). Glioblastoma multiforme (GBM), the most frequent, deadliest, and most malignant form of glioma, has one of the highest mortality rate among human cancers. Chemotherapy with a variety of agents, such as DNA-damaging alkylators temozolomide, 1,3-bis(2-chloroethyl)-1-nitrosourea (BCNU), 1-(2-chloroethyl)-3-cyclohexyl-L-nitrosourea, carboplatin, and cisplatin, has yielded only modest effects (1). Consequently, targeted therapy has attracted much attention as an alternative therapeutic strategy to treat malignant gliomas, such as those targeting epidermal growth factor receptor (EGFR), EGFRvIII, HER2, bcr-abl, vascular endothelial growth factor (VEGF), mammalian target of rapamycin, platelet-derived growth factor, and histone deacetylase (2, 3).

Medulloblastomas are the most common brain tumors in childhood (4). Medulloblastoma therapy remains modestly effective in which conventional surgery/radiation approaches are effective in shrinking primary medulloblastomas. However, recurrence, metastasis, and unwanted side effects are common (4, 5). Several chemotherapy trials have been carried out aiming to improve the modest survival rate of 50% (6). Unfortunately, toxicity is a major setback of not only radiation but also high-dose chemotherapy and the effects can be long term and devastating. Thus, more effective and less toxic therapy is urgently needed for children with medulloblastomas.

Authors' Affiliation: Department of Surgery, Duke University, Duke Comprehensive Cancer Center, and Robert Tisch Brain Tumor Center, Durham, North Carolina

Received 11/19/07; revised 5/30/08; accepted 5/30/08.

Grant support: NIH grant 5K01-CA118423-02 (H-W. Lo), Robert Tisch Brain Tumor Center at Duke University, Duke Brain Cancer Specialized Program of Research Excellence (NIH) Career Development Award (H-W. Lo), Pediatric Brain Tumor Foundation (H-W. Lo), Elsa U. Pardee Foundation (H-W. Lo), and Duke Comprehensive Cancer Center Core Grant (NIH).

The costs of publication of this article were defrayed in part by the payment of page charges. This article must therefore be hereby marked *advertisement* in accordance with 18 U.S.C. Section 1734 solely to indicate this fact.

Note: Supplementary data for this article are available at Clinical Cancer Research Online (http://clincancerres.aacrjournals.org/).

Requests for reprints: Hui-Wen Lo, Department of Surgery (Box 3156), Duke University, 433A MSRB I, 103 Research Drive, Durham, NC 27710. Phone: 919-668-6792; Fax: 919-684-5483; E-mail: huiwen.lo@duke.edu.

doi:10.1158/1078-0432.CCR-07-4923

Translational Relevance

Malignant gliomas and medulloblastomas are the most common brain tumors in adults and children, respectively. Unfortunately, glioblastomas are one of the most lethal malignancies and the treatments for which require urgent improvement. As for medulloblastomas, their therapy remains modestly effective; however, recurrence, metastasis, and unwanted side effects are frequent. Therefore, more effective and less toxic therapy is urgently needed for patients with these brain malignancies. Importantly, the results from this study provide new rationales for novel combinational therapies using anti-STAT3/JAK2 agents to sensitize EGFR/EGFRvIII-expressing malignant gliomas to anti-EGFR agents and to synergistically cooperate with the alkylating agent cisplatin in targeting medulloblastoma and malignant glioma cells. These findings also prompt the need of a future evaluation of the therapeutic efficacy of STAT3-based combinational therapy in targeting high-grade/malignant gliomas and medulloblastomas.

Signal transducer and activator of transcription 3 (STAT3) is an oncogenic transcription factor (7, 8) that is constitutively active in many human cancers (9–11) and regulates the transcription of several genes that are involved in cell cycle progression, antiapoptosis, cell survival, and angiogenesis, such as *cyclin D1*, *c-fos*, *c-Myc*, *pim-1*, *Bcl-XL*, *VEGF*, and *MMP-2* (12–20). STAT3 can be activated by EGFR, JAK2, and other tyrosine kinases whose activation can be mediated by EGF, leukemia inhibitory factor (LIF), and other cytokines (7, 8, 21). Thus, STAT3 is a convergent point of many signaling pathways and has a major role in oncogenesis (22) and tumor metastasis (23), and efforts are ongoing to target it in anticancer drug development (24, 25). STAT3 has also been shown to be constitutively activated in gliomas (26, 27) and medulloblastomas (26, 28); however, its association with high-grade gliomas, primary/*de novo* or secondary through progression from low-grade gliomas, remains uninvestigated. The first generation of anti-JAK2/STAT3 therapeutics is currently being evaluated in preclinical models of various cancer types (29–31) and showed promising results in targeting malignant gliomas (32). However, the efficacy of anti-JAK2/STAT3 strategies in medulloblastomas has not been evaluated. Also unaddressed is whether anti-JAK2/STAT3 agents cooperate with other chemotherapeutic agents to target human malignant gliomas and medulloblastomas.

The gene encoding EGFR and its constitutively activated variant, EGFRvIII, are often amplified and overexpressed in human adult gliomas (33, 34). In contrast, EGFR and EGFRvIII are not significantly involved in medulloblastomas (35). EGFRvIII is a product of rearrangement with an in-frame deletion of 801 bp of the coding sequence of the extracellular domain, resulting in a deletion of residues 6 to 273 and a glycine insertion as residue 6 (34, 36–38). Both EGFR and EGFRvIII are tumorigenic for gliomas and major targets for glioma therapy (2, 39). Unfortunately, anti-EGFR/EGFRvIII therapy remains unsatisfactory in targeting malignant gliomas. The efficacy of anti-EGFR small-molecule inhibitors and monoclonal antibodies in treating glioma patients has been evaluated in clinical trials as single agent and in combination with other chemotherapeutic agents but showed only modest effects (2, 40, 41). Given the insufficient clinical efficacy and limited knowledge of the mechanisms underlying resistance to anti-EGFR therapy, a major goal of this study is to better our understanding of the malignant biology of EGFR-expressing gliomas and to elucidate the cellular factors that drive the resistant phenotype in these tumors.

Mechanisms underlying the resistance of human cancers to anti-EGFR therapy remain unclear. Nevertheless, PTEN mutation and deregulated phosphatidylinositol 3-kinase pathway have been shown to correlate positively with resistance of GBM patients to EGFR inhibitors (41, 42). We and others reported that STAT3 physically interacted and functionally cooperated with EGFR, at both cytoplasmic and nuclear levels, to induce gene expression and regulate important cellular processes (9, 43). On the cell surface, activated EGFR recruits and phosphorylates STAT3 at Y705, and in turn, phosphorylated STAT3 (p-STAT3) enters the nucleus to activate expression of several cancer-related genes (43). We have recently shown that EGFR cooperates with STAT3 to induce TWIST expression and facilitate epithelial-mesenchymal transition in human breast and epidermoid carcinomas, epithelial cancers (11). In the nucleus, EGFR interacts with STAT3 to activate expression of inducible nitric oxide synthase (9). Moreover, dual inhibition of EGFR, JAK2, and JAK2/STAT3 led to a synergistic killing of EGFR/p-STAT3–expressing human breast and epidermoid carcinoma cells (9). Moreover, EGFR and JAK2 do significantly cross-talk. EGFR interacts with and phosphorylates JAK2 leading to JAK2 activation. On the other hand, JAK2 can phosphorylate EGFR to activate the mitogen-activated protein kinase pathway (44). Together, these findings revealed that deregulated EGFR and STAT3 pathways significantly cross-talk at multilevels, leading to more aggressive tumor behaviors. However, the effect of these cross-talks on malignant gliomas remains uninvestigated.

In this study, we found a high extent of STAT3 constitutive activation in primary glioma specimens, particularly in high-grade/malignant gliomas, and cultured malignant glioma and medulloblastoma cells, and the extent of STAT3 constitutive activation correlated positively and significantly with glioma grade. These findings prompted us to examine whether inhibition of STAT3 alone led to medulloblastoma and malignant glioma cell death. In light of the role of EGFR as a STAT3-activating kinase, we further examined whether EGFR and constitutively activated STAT3 coexisted in primary glioma specimens and elucidated the pathologic significance of this coexpression in gliomas. Finally, we addressed whether inhibitors to EGFR and JAK2/STAT3 synergistically targeted EGFR- and EGFRvIII-expressing human GBM cells and if the anti-JAK2/STAT3 agent sensitized malignant glioma and medulloblastoma cells to clinically used chemotherapeutic agents, such as DNA-damaging alkylating agents.

Materials and Methods

Primary specimens and cell lines. Human medulloblastoma (UW228) and malignant glioma cell lines (anaplastic astrocytoma MGR1 and UW5 cells; GBM MGR2, MGR3, UW14, and UW281 cells)

Table 1. Constitutive activation of STAT3 positively and significantly correlates with glioma grade

	p-STAT3 < 20%	p-STAT3 ≥ 20%	% specimens with constitutively activated STAT3
Normal brain	4*	1	20.0% (1/5)
Astrocytoma I	8	3	27.3% (3/11)
Astrocytoma II	17	7	29.2% (7/24)
Astrocytoma III	6	8	57.1% (8/14)
Astrocytoma IV/GBM	2	4	66.7% (4/6)
All gliomas, *n*	33	22	40.0% (22/55)

NOTE: The extent of STAT3 activation in primary brain tumors and adjacent normal tissues was measured by immunohistochemical staining of a tissue array slide for p-STAT3 (Y705) and the correlation between STAT3 constitutive activation and glioma grade was subsequently determined. Immunostained normal brain tissues (n = 5) and gliomas (n = 55) were grouped into two categories according to a well-established system (48, 49): p-STAT3 ≥ 20% (regarded as constitutive activation) and p-STAT3 < 20%. Regression analysis was done to determine the relationship between STAT3 constitutive activation and glioma grade (P = 0.0136; R = 0.949).
*Number of specimens.

were established from primary specimens (45). U87MG human GBM cells and mouse normal astrocytes, C8-S (type II phenotype) and C8-D30 (type III phenotype), were obtained from the American Type Culture Collection. U87MG-vector, U87MG-EGFR, and U87MG-EGFR-vIII stable cell lines were established from the U87MG cells that expressed very low levels of wild-type EGFR. All cells were maintained in DMEM supplemented with 10% FCS. The stable U87MG cells were additionally supplemented with 1 mg/mL G418.

Reagents and chemicals. All chemicals and biochemicals were purchased from Sigma unless otherwise stated. Rabbit polyclonal antibodies to EGFR, cyclin D1, VEGF, JAK2, and STAT3 were purchased from Santa Cruz Biotechnology. Mouse monoclonal β-actin and α-tubulin antibodies were from Sigma. Rabbit polyclonal, p-STAT3 (Y705), phosphorylated JAK2 (p-JAK2; Y1007/1008), and phosphorylated EGFR (Y1045) antibodies were from Cell Signaling. Mouse monoclonal Myc-tag antibody was from Roche. The GAS luciferase vector, pGAS-Luc, was purchased from Stratagene. Dual Luciferase Assay and CellTiter Blue Cell Viability Assay kits were from Promega. JSI-124 was obtained from NIH and EMD Chemicals. EGFR and EGFRvIII expression vectors were generated from pCMV-Tag5A (Stratagene) by cloning the cDNAs into the *Hin*dIII and *Xho*I sites of the vector. Both EGFR and EGFRvIII were expressed as Myc-tagged fusion proteins. LIF was purchased from EMD Chemicals. Consecutive tissue array slides were obtained from Imgenex and reagents used for immunohistochemical staining were from Vector Laboratories.

Immunohistochemical staining of primary specimens for p-STAT3 and EGFR. The immunoperoxidase staining method used in these studies was a modification of the avidin-biotin complex technique, as described previously (46). The tissue array (Imgenex) contained paraffin-embedded microsections (5 μm) of 63 cases, including 5 normal brain tissues, 11 astrocytoma I, 24 astrocytoma II, 14 astrocytoma III, 6 astrocytoma IV/GBM, 2 medulloblastomas, and 1 ependymoma. The tumor sections were deparaffinized, dehydrated, and subjected to antigen retrieval in a microwave oven followed by incubation with 0.05% trypsin in PBS for 15 min at room temperature. Endogenous peroxidase activity was blocked by treatment of 0.3% hydrogen peroxide, and the slides were incubated with 10% normal goat serum for 30 min and then with the p-STAT3 antibody (1:30; Cell Signaling) and EGFR antibody (1:50; Novocastra) at 4°C overnight. Following washes with PBS, the slides were incubated with biotinylated secondary antibodies and then with avidin-biotin-horseradish peroxidase complex. Detection was done using 0.125% aminoethylcarbazole chromogen. After counterstaining with Mayer's hematoxylin (Sigma), the slides were mounted. Scoring was done by a pathologist.

Western blot analysis. Whole-cell lysates were extracted from cultured cells via sonication, electrophoresed onto SDS-polyacrylamide gels, and transferred to polyvinylidene difluoride membranes, as previously described (9). Membranes were incubated with antibodies, including rabbit polyclonal EGFR, phosphorylated EGFR (Y1045), STAT3, p-STAT3 (Y705), cyclin D1, JAK2, p-JAK2 (Y1007/1008), and VEGF antibodies as well as mouse monoclonal β-actin and α-tubulin antibodies.

Immunofluorescence staining and confocal microscopy. Tumor cells and normal astrocytes were seeded in eight-well Lab-Tek chamber slides (Nunc, Inc.) for 24 h. After washing with ice-cold PBS, the cells were fixed in 4% paraformaldehyde for 15 min and permeabilized with 0.2% Triton X-100 for 5 min. Following treatment with 10% normal goat serum/1% bovine serum albumin for 60 min, the cells were incubated with polyclonal rabbit p-STAT3 and Myc-tag antibodies overnight at 4°C. After three washes with PBS, the cells were incubated with goat anti-rabbit secondary antibody (1:200; Vector Laboratories) tagged with fluorescein, and after which, they were mounted with Vectashield Mounting Medium containing propidium iodide (for nuclei detection) and then examined under a Zeiss LSM 510 confocal microscope. In LIF studies, cells were serum starved for 16 h and treated without and with 100 ng/mL LIF for 15 min and subjected to immunofluorescence staining and confocal microscopy.

Transfection and luciferase assay. Luciferase constructs used in these studies were pGAS-Luc and pcyclin D1-Luc, a generous gift from Dr. Mien-Chie Hung (M. D. Anderson Cancer Center, Houston, TX). All transfections were done with cells in exponential growth using Lipofectamine LTX (Invitrogen) and FuGENE HD (Roche). A *Renilla* luciferase expression vector, pRL-CMV, whose expression is controlled by the CMV promoter was used to control for transfection efficiency. Forty-eight hours after transfection, the cells were lysed and luciferase activity was measured using the Dual Luciferase Assay kit in a TD 20/20 luminometer (Promega), as previously described (9). Relative luciferase activity was calculated by normalization of the firefly luciferase activity against that of the *Renilla* luciferase.

Cell survival and clonogenic growth assays. Tumor cells and normal astrocytes in exponential growth were seeded in 96-well culture plates and treated with vehicle control (1% DMSO) and various agents. After 48 h, the cells were subjected to cell survival analyses using the CellTiter Blue Cell Viability Assay. Briefly, 25 μL of the CellTiter Blue reagent were added to each well containing 100 μL medium and incubated for 4 h at 37°C, and then the absorbance was measured at 560/590 nm using a plate reader (Synergy-HT, Bio-Tek). Clonogenic growth assay was done in six-well cell culture plates with 250 to 2,000 cells seeded per well, as previously described (9). Seeded cells were treated with 0 to 1 μmol/L of JSI-124 for 24 h, and medium was removed and replaced with fresh drug-free growth medium for 10 to 14 d. Colonies were stained with crystal violet blue solution (Sigma) for 1 h, washed with water, dried, and counted. Triplicate wells were used for each treatment and three independent experiments were done to derive means and SDs.

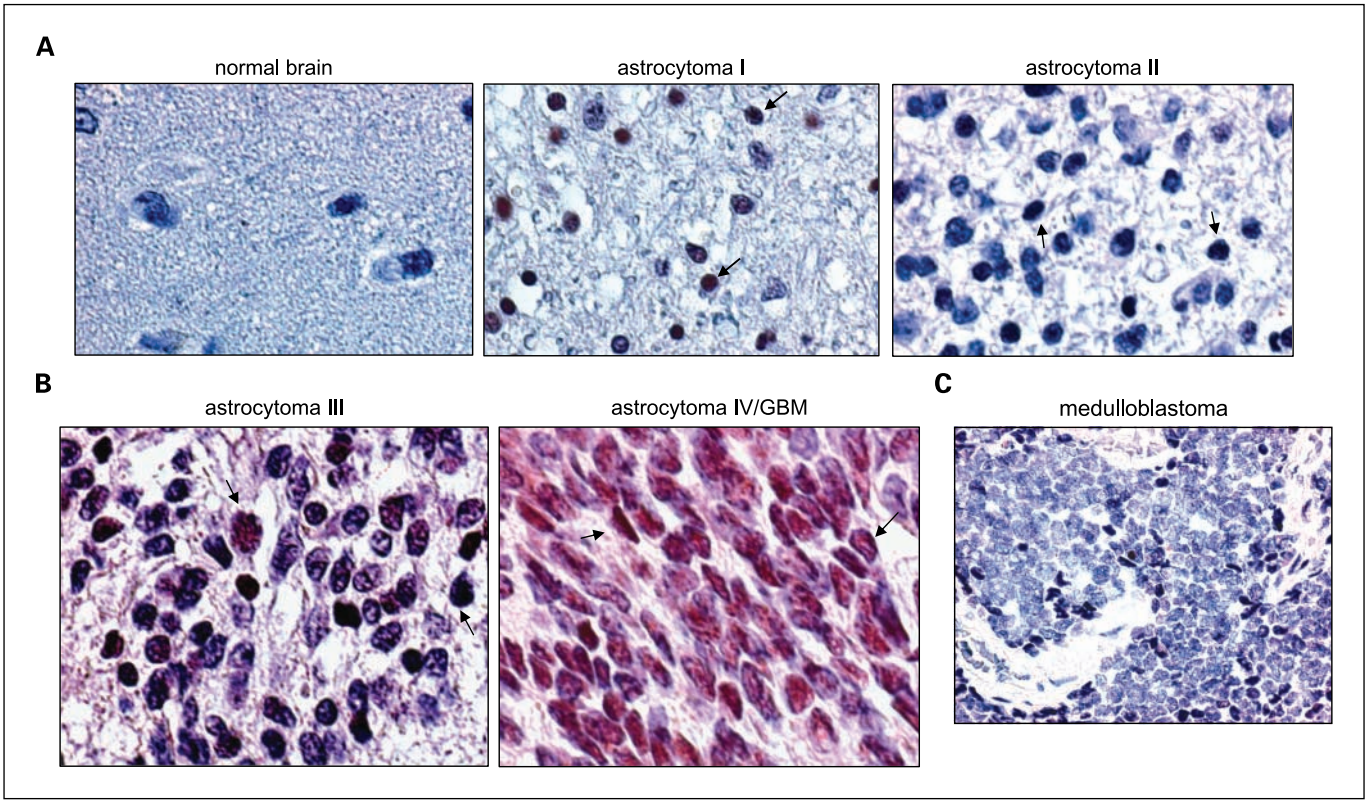

Fig. 1. Constitutive activation of STAT3 was detected in primary glioma and medulloblastoma specimens. The extent of STAT3 activation in primary brain tumors and adjacent normal tissues was measured by immunohistochemical staining of a tissue array slide for p-STAT3 (Y705). *A* and *B,* representative immunostained cases. *A,* normal brain tissue, grade 1 astrocytoma, and grade 2 astrocytoma. *B,* high-grade gliomas, grade 3 astrocytoma/anaplastic astrocytoma, and grade 4 astrocytoma/GBM. Arrows point to p-STAT3 – positive nuclei that were brown/dark red, whereas p-STAT3 – negative nuclei were light blue as we previously described (11). *C,* a representative medulloblastoma from a 3-y-old patient that was immunostained positively for p-STAT3.

Measurement of apoptosis. Cells treated per experimental procedures were harvested using trypsin-EDTA, washed with DMEM, and fixed in DMEM and ethanol (1:1) at 4°C. Fixed cells were pelleted, washed with growth medium, treated with RNase A (1 mg/mL in PBS), and stained with propidium iodide (50 μg/mL in PBS). Cell cycle phase distribution was determined using an EPICS Profile II flow cytometer (Coulter Electronics). Cells at the sub-G_1 phase are considered the apoptotic population.

Median-effect analysis for treatment synergy. To determine the efficacy of Iressa and JSI-124 combinations, tumor cells were treated with 0 to 100 μmol/L of Iressa, 0 to 10 μmol/L of JSI-124, or 12.5 μmol/L Iressa plus 0.1, 0.5, or 1.0 μmol/L of JSI-124 for 48 h. To determine the effect of JSI-124/cisplatin combinations, tumor cells were treated with 0 to 200 μmol/L of cisplatin, 0 to 1 μmol/L of JSI-124, or in combination with a 200:1 molar ratio (cisplatin/JSI-124) for 48 h. Survival fractions in each treatment were determined by CellTiter Blue Cell Viability Assay described above and the combination index (CI) was computed using the method developed by Chou and Talalay (47) and the computer software CalcuSyn (Biosoft).

Statistical analysis. Regression analysis and Student's *t* test were conducted using STATISTICA (StatSoft) and Microsoft Excel. $P < 0.05$ was considered statistically significant.

Table 2. Characteristics of all cell lines used in this study

Cell lines	Cell types
MGR3	GBM
MGR1	Anaplastic astrocytoma
UW281	GBM
UW228	Medulloblastoma
MGR2	GBM
UW14	GBM
U87MG	GBM
C8-S	Astrocytes
C8-D30	Astrocytes

Results

STAT3 constitutive activation was frequently detected in primary high-grade/malignant gliomas and correlated significantly and positively with glioma grade. While the relationship of STAT3 constitutive activation with glioma grade remains elusive, we aimed to determine the extent of STAT3 activation in primary human glioma specimens by immunostaining a tissue array slide for p-STAT3 (Y705), the active phosphorylated form of STAT3, and correlated the extent with glioma grade. STAT3 constitutive activation was defined as ≥20% of the cells in the tumor section staining positive for p-STAT3 (9, 48, 49). As shown in Table 1, the frequency of constitutively activated STAT3 was very low (1 of 5, 20%) in normal brain tissues and higher in gliomas (22 of 55, 40%). In gliomas, the extent of STAT3 constitutive activation was 27.3%, 29.2%, 57.1%, and 66.7% in

astrocytoma grades I, II, III (anaplastic astrocytoma), and IV (GBM), respectively. Among the 55 glioma specimens analyzed, STAT3 was constitutively activated in 28.6% (10 of 35) of the low-grade (grades I and II) and 60% (12 of 20) in high-grade/malignant (grades III and IV) gliomas. Regression analysis further indicated a significant positive correlation between STAT3 constitutive activation and glioma grade ($P = 0.0136$; $R = 0.949$). Representative immunostained slides are shown in Fig. 1A and B, in which arrows point to nuclei that were stained positive for p-STAT3. Nuclei immunostained positive for p-STAT3 were indicated as brown/dark red signals, in contrast to the light blue p-STAT3 – negative nuclei, as we previously described (9, 11). Normal brain tissue in Fig. 1A showed negative p-STAT3 staining, whereas glioma samples used were positively stained for p-STAT3. A medulloblastoma (Fig. 1C) and an ependymoma (data not shown) were also positive for p-STAT3. Together, these results indicate that constitutive activation of STAT3 is a frequent occurrence in human high-grade/malignant gliomas and is positively associated with glioma grade.

STAT3 and JAK2 were constitutively activated in cultured human malignant glioma and medulloblastoma cells. To better understand the extent of STAT3 activation in malignant gliomas and medulloblastomas, we analyzed four human malignant glioma and the medulloblastoma UW228 cell lines for the extent of STAT3 activation by determining the level of p-STAT3. Characteristics of all cell lines are described in Table 2. Indeed, p-STAT3 was expressed at high levels in all five cell lines that we analyzed (Fig. 2A). In contrast, normal astrocytes, C8-S and C8-D30, did not express any detectable levels of STAT3 (Fig. 2B). Stimulation with a STAT3-activating cytokine LIF did not result in STAT3 phosphorylation in C8-S and C8-D30 cells (Supplementary Fig. S1). To elucidate the upstream kinases that phosphorylate/activate STAT3 in these cells, we analyzed the levels of EGFR (Fig. 2A) and JAK2/p-JAK2 (Fig. 2C), two tyrosine kinases that phosphorylate STAT3 at Y705. It is noticeable that only UW14 GBM cells contained significant levels of endogenous EGFR, which is consistent with the notion that primary gliomas tend to lose EGFR/EGFRvIII expression after culturing *in vitro* (50) and that medulloblastomas do not express detectable levels of EGFR (35). These cells contained intrinsic active JAK2 (Fig. 2C), p-JAK2 (Y1007/1008), indicating that constitutively activated JAK2 may contribute to the observed constitutive activation of STAT3 in cultured human malignant glioma and medulloblastoma cells.

Nuclear expression of p-STAT3, an indication for active STAT3 as a transcription factor, in human malignant glioma and medulloblastoma cell lines was further analyzed using immunofluorescence staining and confocal microscopy (Fig. 3). Nuclear p-STAT3 is indicated as yellow signals, merged products of p-STAT3 (green) and nuclei (red from propidium iodine). Here, we detected significant nuclear localization of p-STAT3 in UW228 medulloblastoma cells (Fig. 3A) and GBM lines (MGR3 cells in Fig. 3B; three additional lines not shown). In contrast, normal astrocytes contained very low levels of p-STAT3 (Fig. 3C). Consistent with the observed high levels of p-STAT3 in the cell nucleus, malignant glioma and medulloblastoma cell lines showed a significantly higher ability to activate STAT3 target promoters, the gamma-activated sequence/GAS-containing (*left*) and *cyclin D1* (*right*) promoters, than normal astrocytes (Fig. 3D). To note,

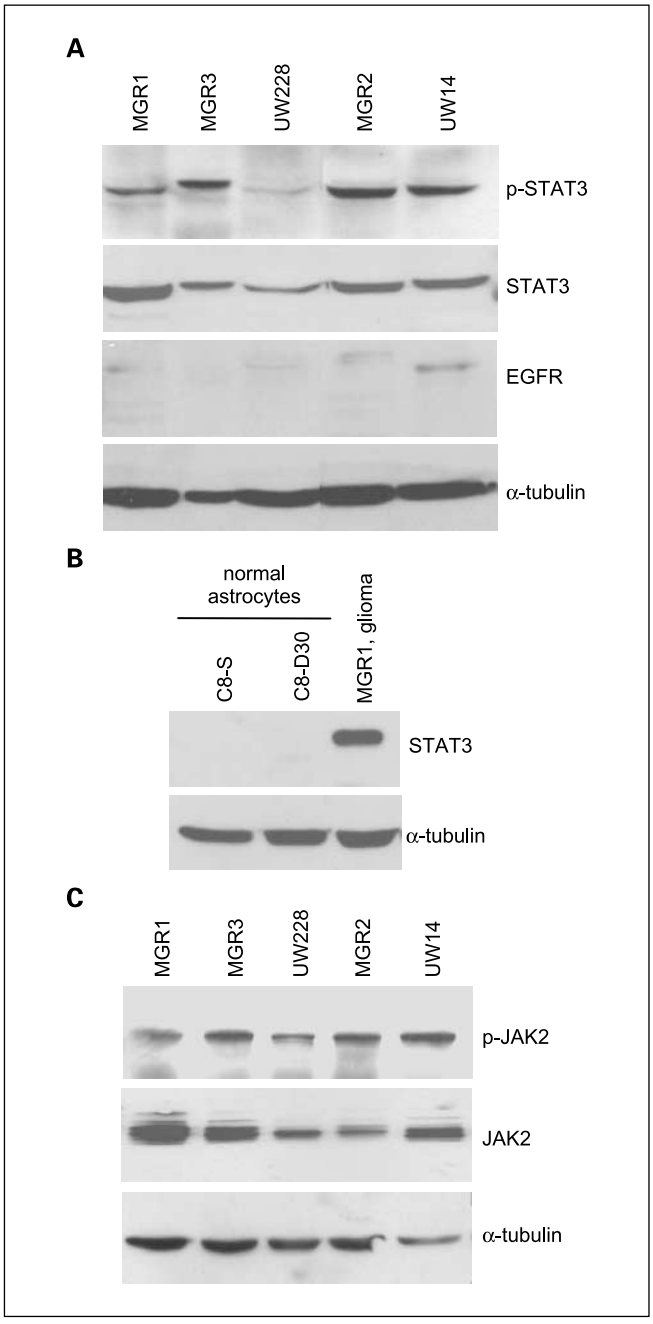

Fig. 2. STAT3 and JAK2 constitutive activation was observed in cultured human medulloblastoma and malignant glioma cells but not in normal astrocytes. *A,* human malignant glioma and medulloblastoma cells frequently expressed constitutively activated STAT3 (*p-STAT3*). Human malignant glioma (MGR1, MGR3, MGR2, and UW14) and medulloblastoma UW228 cells were analyzed via Western blot analyses for the levels of STAT3, p-STAT3, and EGFR. Levels of α-tubulin were also determined as loading controls. *B,* normal astrocytes did not express detectable levels of STAT3 and p-STAT3. Normal astrocytes, C8-S and C8-D30, were lysed, and proteins were extracted and subjected to Western blot analyses to detect STAT3 in which α-tubulin served as a loading control. MGR1 lysates were included as a positive control for STAT3 expression. *C,* JAK2 was found constitutively activated in cultured human medulloblastoma and malignant glioma cells. Tumor cells were analyzed via Western blot analyses for the levels of p-JAK2 (Y1007/1008) and total JAK2. Levels of α-tubulin were also determined as loading controls.

p-STAT3 binds to the GAS motif within the promoters of its downstream target genes to activate their expression (51). Moreover, similar levels of p-STAT3 were detected in the control and LIF-treated MGR3 GBM cells (Supplementary Fig. S2),

suggesting LIF-independent STAT3 activation in these cells. This is consistent with the notion that LIF is not significantly involved in STAT3 activation in glioma cells (52). Together, these data indicate that the STAT3 pathway, including its upstream tyrosine kinase JAK2 and downstream gene targets, is constitutively activated in human malignant glioma and medulloblastoma cells.

JAK2/STAT3 inhibition robustly targeted human medulloblastoma and high-grade/malignant glioma cells. The efficacy of anti-STAT3 approaches in targeting medulloblastomas has yet been evaluated, whereas gliomas are targeted by small-molecule inhibitors, dominant-negative STAT3, and STAT3 small interfering RNA (32, 53, 54). In light of our observation that STAT3 is frequently activated in cell lines and primary specimens of human medulloblastomas and gliomas, we hypothesized that STAT3 activation is important for the growth of these cells and that STAT3 suppression will lead to their death. It is also worthwhile to mention that the efficacy of a small-molecule JAK2/STAT3 inhibitor, JSI-124/cucurbitacin I, in targeting glioma and medulloblastoma cells has yet been evaluated, to our best knowledge. As shown in Fig. 4A, 48-h treatments with JSI-124 resulted in a dose-dependent growth suppression of medulloblastoma and malignant glioma cells. IC_{50} values for JSI-124 were significantly lower, 0.006 to 0.05 μmol/L, for medulloblastoma and malignant glioma cells than 0.5 μmol/L for normal astrocytes, indicating that JSI-124 specifically targeted these tumor cells but not normal astrocytes. Consistently, JSI-124 IC_{50} values in C8-D30 normal astrocytes were 22- to 83-fold higher than those in human glioma and medulloblastoma cells. The observed potent JSI-124–mediated growth suppression in both medulloblastoma and malignant glioma cells was further confirmed using clonogenic growth assay (Fig. 4B). Because STAT3 suppression has been shown to induce apoptotic cell death, we next examined whether JSI-124 killed these tumor cells, in part, via induction of apoptosis and found that all five medulloblastoma and high-grade glioma cell

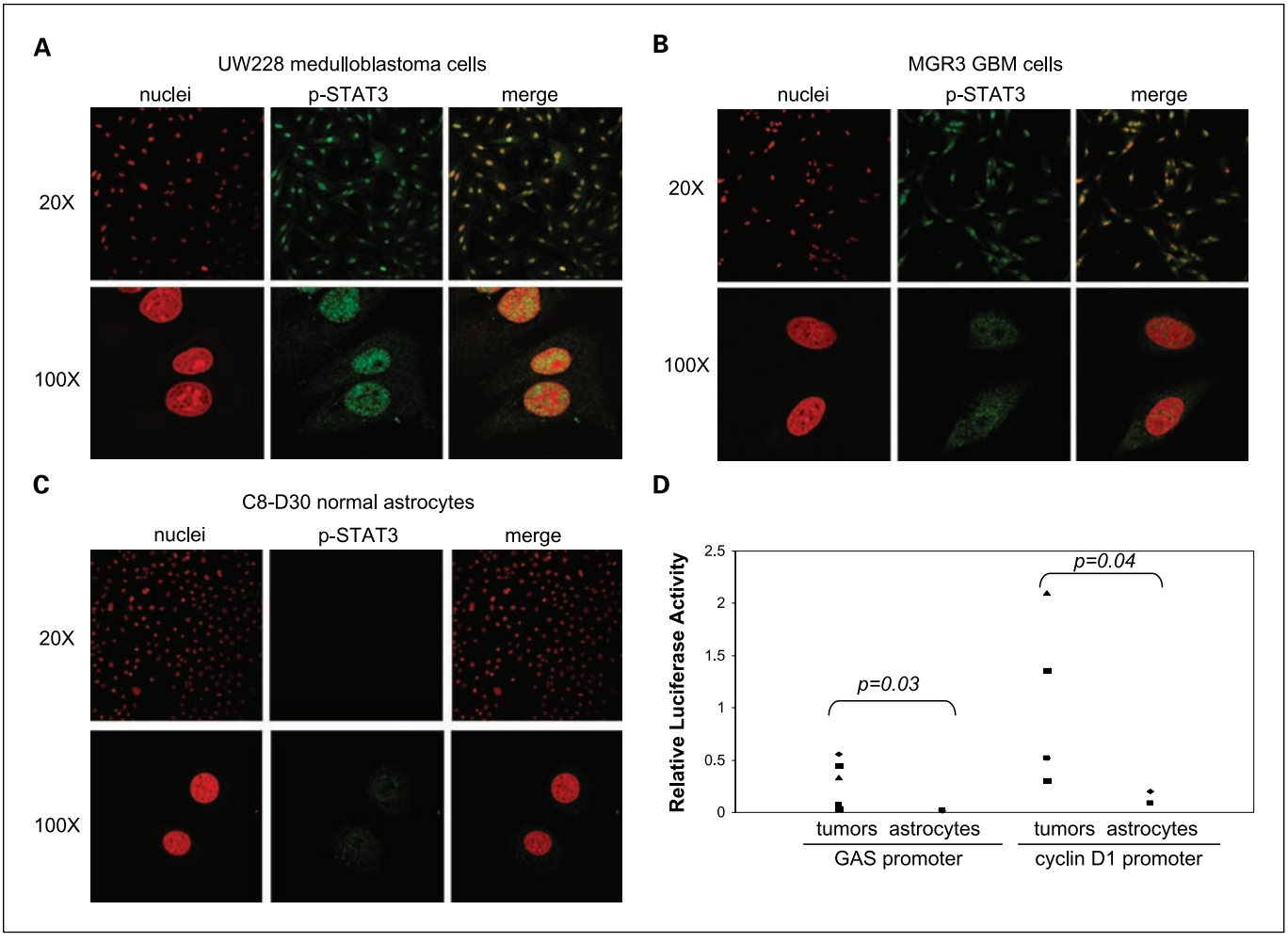

Fig. 3. Nuclear expression and transcriptional activity of activated STAT3 were detected in human malignant glioma and medulloblastoma cells. The medulloblastoma UW228, human GBM MGR3 cells, and two normal astrocytes, C8-S and C8-D30, were used in these studies. *A* to *C,* high levels of p-STAT3 in the nucleus of tumor cells but not normal astrocytes. Immunofluorescent staining and confocal microscopy analysis were conducted to indicate p-STAT3 expression and cellular location. Nuclear p-STAT3 was identified using anti-p-STAT3 antibody, whereas nuclei were stained with propidium iodine and indicated as red signals. Nuclear p-STAT3 was shown as yellow signals, merged products of p-STAT3 (*green*) and nuclei (*red*). Low (×20) and high (×100) resolution images for medulloblastoma (*A*), malignant glioblastoma MGR3 cells (*B*), and normal astrocytes (*C*) are shown. *D,* high STAT3 activity in medulloblastoma and malignant glioma cells but not in normal astrocytes. Tumor cells and normal astrocytes were transfected with pGAS-Luc or pcyclin D1-Luc and the control vector pRL-TK. Following 48 h, cells were lysed and subjected to luciferase assay as we previously described (9, 11). All data were derived from three independent experiments and analyzed by the Student's *t* test for *P* values.

lines underwent significant apoptosis following JSI-124 treatments (Fig. 4C).

To examine whether JSI-124 targeted these cancer cells by specific inhibition of STAT3 activation, we examined the effects of JSI-124 on STAT3 phosphorylation at Y705 and the expression of STAT3 target genes, *cyclin D1* and *VEGF*. JSI-124 time-dependently reduced p-STAT3 levels in both MGR1 human anaplastic astrocytoma (Fig. 4D) and MGR3 human GBM cells (Supplementary Fig. S3). We also observed a time-dependent reduction in the expression of cyclin D1 and VEGF in MGR1 cells (Fig. 4D). In MGR3 cells, cyclin D1 levels time-dependently decreased after JSI-124 treatments (Supplementary Fig. S3). To note, MGR3 cells did not contain detectable levels of VEGF, which is in contrast to other human malignant gliomas that express high levels of VEGF (data not shown). Consistently, JSI-124 significantly reduced the ability of STAT3 to activate both *cyclin D1* and GAS-containing promoters in MGR1 (Fig. 4D) and MGR3

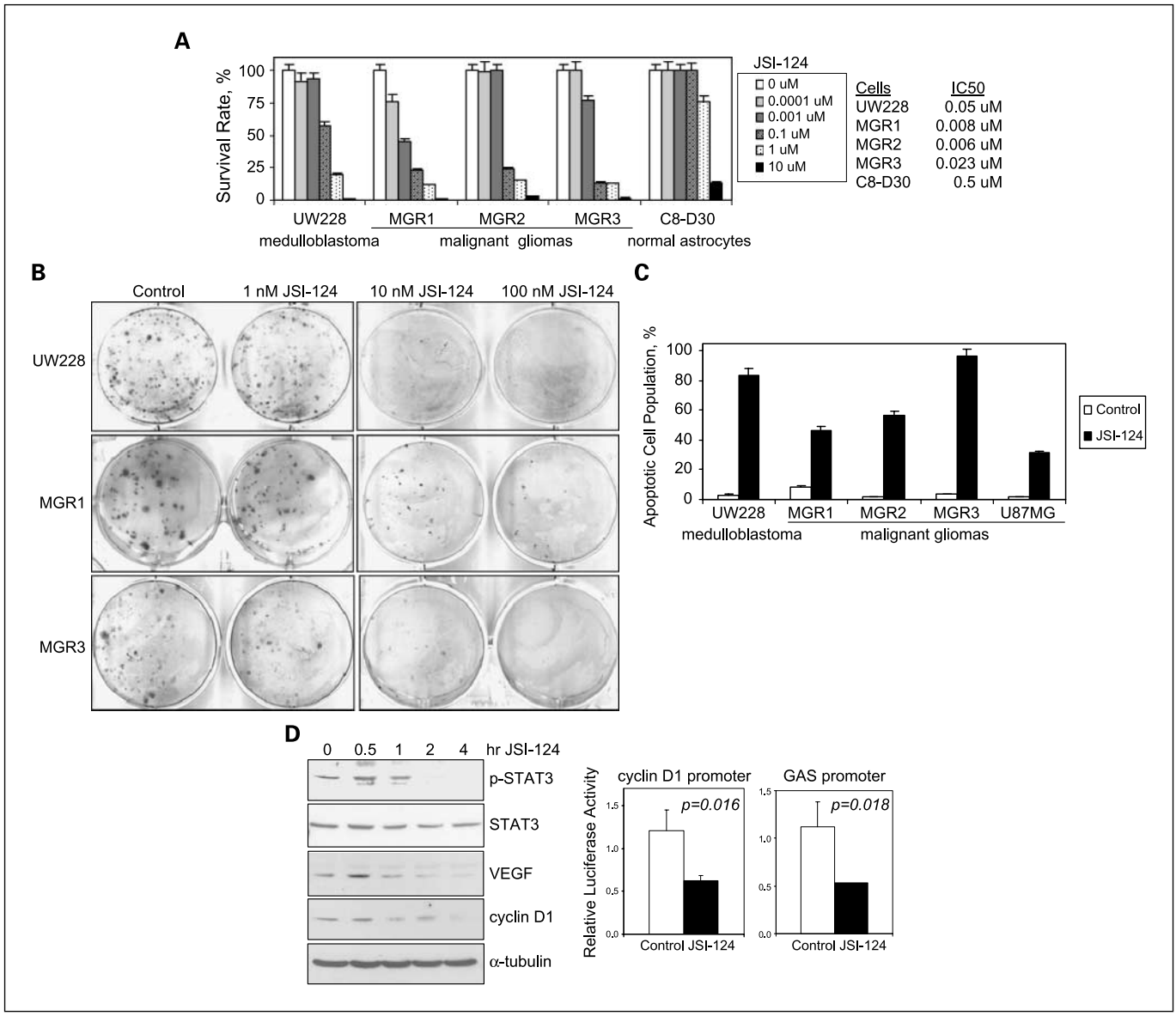

Fig. 4. JAK2/STAT3 inhibition by JSI-124 robustly suppressed STAT3 activation, reduced expression of its target genes, and killed human medulloblastoma and malignant glioma cells. *A,* a small-molecule inhibitor for JAK2/STAT3, JSI-124, strongly inhibited the growth of medulloblastoma UW228 and malignant glioma (MGR1, MGR2, and MGR3) cells but not normal astrocytes. JSI-124 has been previously tested to have JAK2/STAT3 inhibitory effects (25). All cells were treated with JSI-124, 0 to 10 μmol/L, for 48 h; cell viability was determined; and IC_{50} values were derived. *B,* the killing effect of JSI-124 was confirmed using the clonogenic growth assay. UW228, MGR1, and MGR3 cells in single-cell suspension were seeded in triplicates onto six-well culture plates 24 h before JSI-124 treatments, exposed to JSI-124 (0-100 nmol/L) for 24 h, and then cultured in regular growth medium. Colonies were stained with crystal violet blue solution and counted 10 to 14 d later. Representative colonies stained with crystal violet blue are shown. *C,* JSI-124 induced significant apoptotic cell death. The medulloblastoma UW228 cell line and four malignant glioma (MGR1, MGR2, MGR3, and U87MG) cell lines were treated with and without JSI-124, 1 μmol/L, for 24 h, harvested, and subjected to cell cycle analyses. Apoptotic cells were indicated by those in the sub-G_1 cell cycle phase. *D,* JSI-124 suppressed STAT3 activation and expression of its downstream target genes, *cyclin D1* and *VEGF*. Left, MGR1 anaplastic astrocytoma cells were treated with 1 μmol/L JSI-124 for 0 to 4 h, harvested, and subjected to Western blot analysis to determine levels of p-STAT3, STAT3, VEGF, cyclin D1, and α-tubulin; right, MGR1 cells were transfected with pGAS-Luc or pcyclin D1-Luc and the transfection efficiency control, pRL-TK. Forty hours after transfection, cells were treated with and without JSI-124 for 4 h, lysed, and subjected to luciferase assay. All data were derived from three independent experiments and analyzed by the Student's *t* test for *P* values.

Table 3. Coexpression of EGFR and constitutively activated STAT3 correlates significantly and positively with glioma grade

	Others*†	EGFR$^+$/p-STAT3 $\geq$ 20%†	% specimens with EGFR$^+$/constitutively activated STAT3
Normal brain	5	0	0% (0/5)
Astrocytoma I	11	0	0% (0/11)
Astrocytoma II	21	3	12.5% (3/24)
Astrocytoma III	11	3	21.3% (3/14)
Astrocytoma IV/GBM	4	2	33.3% (2/6)

NOTE: To examine whether EGFR and constitutively activated STAT3 coexpressed in primary glioma specimens, we further immunostained the cohort of human gliomas, which we previously analyzed for p-STAT3, for EGFR as we previously described (47). Normal brain tissues and gliomas were grouped into two categories according to EGFR and p-STAT3 levels: "EGFR$^+$/p-STAT3 $\geq$ 20%" and "others" that included gliomas with EGFR$^-$/p-STAT3 < 20%, EGFR$^-$/p-STAT3 $\geq$ 20%, and EGFR$^+$/p-STAT3 < 20%. Tissues with p-STAT3 $\geq$ 20% were regarded as with STAT3 constitutive activation (48, 49). Regression analysis was done to determine the relationship between coexpression of EGFR with STAT3 constitutive activation and glioma grade (P = 0.0019; R = 0.99).

*Gliomas with EGFR$^-$/p-STAT3 < 20%, EGFR$^-$/p-STAT3 $\geq$ 20%, and EGFR$^+$/p-STAT3 < 20%.

† Values indicate number of specimens.

(Supplementary Fig. S3) cells. Using isogenic U87MG cell lines, U87MG-vector, and U87MG-EGFR, we found U87MG-EGFR cells to contain significantly higher p-STAT3 expression and a high sensitivity to JSI-124 (Supplementary Fig. S4), relative to U87MG-vector cells, indicating that JSI-124 preferentially targets cancer cells with high p-STAT3. Taken together, these results indicate that the JAK2 inhibitor JSI-124 robustly inhibits STAT3 phosphorylation/activation and reduces expression of its downstream target genes, leading to significant cell death in human medulloblastoma and high-grade/malignant glioma cells.

Coexpression of EGFR and constitutively activated STAT3 was detected in primary glioma specimens and correlated significantly and positively with glioma grade. In light of our observations that STAT3 was constitutively activated in 40% of human primary gliomas and 60% in high-grade/malignant gliomas, and that EGFR and constitutively activated STAT3 were coexpressed in, approximately, 40% of a cohort of human breast carcinomas (11), we then asked whether this coexpression also existed in primary glioma specimens. The same cohort of gliomas that we previously immunostained for p-STAT3 was analyzed for EGFR using immunohistochemical staining analysis (46). Approximately, 33% (2 of 6) of the primary GBM/grade IV astrocytomas contained both STAT3 constitutive activation and EGFR expression, whereas 21.3% (3 of 14) of the grade III/anaplastic astrocytomas expressed them (Table 3). Noticeably, none of the normal brain tissues or grade I astrocytoma contained both EGFR and STAT3 constitutive activation. Importantly, regression analysis showed that the extent of coexpression correlated significantly and positively with glioma grade (P = 0.0019; R = 0.99). A representative GBM tumor containing both EGFR and STAT3 constitutive activation is shown in Fig. 5A. Noticeably, EGFR was primarily located in the cell surface and cytoplasm, whereas p-STAT3 was mostly in the nucleus, consistent with its role as transcription factor. Together, these results indicate that EGFR and STAT3 colocalize and potentially cross-talk in primary high-grade/malignant gliomas and such interaction may play an important role in high-grade but not low-grade gliomas.

Combination of anti-EGFR agent Iressa and anti-JAK2/STAT3 agent JSI-124 synergistically targeted stable EGFR- and EGFRvIII-expressing human GBM cells. As we observed a high level of STAT3 constitutive activation and coexpression of EGFR with p-STAT3 in primary GBM specimens, we speculated that the observed high STAT3 activity may contribute to resistance of EGFR/EGFRvIII-expressing GBMs to anti-EGFR therapy. As primary EGFR/EGFRvIII-expressing GBMs tend to lose EGFR/EGFRvIII expression *in vitro* (50), we aimed to mimic these tumors by generating three isogenic stable EGFR- and EGFRvIII-expressing GBM cell lines from U87MG cells who expressed a very low level of endogenous wild-type EGFR. These lines were designated U87MG-vector, U87MG-EGFR, and U87MG-EGFRvIII. Western blot analysis confirmed the expression of EGFR (170 kDa) and EGFRvIII (145 kDa) in U87MG-EGFR and U87MG-EGFRvIII cells, respectively (Fig. 5B). Noticeably, U87MG-EGFR and U87MG-EGFRvIII cells not only expressed high levels of EGFR/EGFRvIII but also p-STAT3, which mimic primary GBMs that coexpress EGFR/EGFRvIII and constitutively activated STAT3, as we observed in 33% of the primary GBMs that we analyzed. These cell lines were then used for subsequent studies.

We found the isogenic stable cell lines to be more resistant to the EGFR kinase inhibitor Iressa compared with the JAK2/STAT3 inhibitor JSI-124 (Fig. 5C). Among these three stable lines, U87MG-vector cells were the least sensitive to both agents, suggesting specific targeting of Iressa to EGFR/EGFRvIII-expressing cancer cells, and JSI-124 to those with high p-STAT3. We then asked whether JSI-124 would sensitize U87MG-EGFR and U87MG-EGFRvIII cells to Iressa treatments and found that combination of Iressa and JSI-124, in the molar ratios of 125:1, 125:5, and 125:10, significantly increased cell kill in both cell lines (Fig. 5D). Iressa and JSI-124 alone did not completely reduce EGF-induced STAT3 activation in U87MG-EGFR cells despite that Iressa successfully inhibited EGF-induced EGFR activation by means of EGFR autophosphorylation at Y1045 (Supplementary Fig. S5A). In contrast, the combination of Iressa and JSI-124 synergistically and significantly decreased p-STAT3 levels. JSI-124 specifically inhibited JAK2/STAT3 pathway rather than EGFR activity. To address whether a treatment synergy existed, we did the median-effect analysis, developed by Chou and Talalay (47), as we previously described (9). The analysis generates CI that indicates synergistic (CI < 1), additive (CI = 1), and antagonistic (CI > 1) effects. It is evidenced by the results shown in

Supplementary Fig. S5B that Iressa and JSI-124 synergistically targeted both U87MG-EGFR and U87MG-EGFRvIII cells at molar ratios of 125:1 and 125:5, but not 125:10, as indicated by CI values that were <1.0. Collectively, these results indicate that high STAT3 activity may constitute a mechanism underlying resistance of human GBMs to anti-EGFR therapy and that dual inhibition of both EGFR and STAT3/JAK2 pathways potently and synergistically targets EGFR- and EGFRvIII-expressing human GBM cells.

JAK2/STAT3 inhibition sensitized malignant glioma and medulloblastoma cells to anticancer agents. Although JAK2/STAT3 suppression targeted malignant glioma cells as shown by this study and other reports (32, 53, 54), its role in sensitizing these tumors to chemotherapeutic agents remains uninvestigated. We showed in this study, for the first time, that STAT3/JAK2 inhibition led to growth suppression of human medulloblastoma cells, which prompted the need to investigate whether such inhibition sensitized these cells to chemotherapeutic agents. Temozolomide, BCNU, and cisplatin are DNA-damaging alkylators and among the most commonly used chemotherapeutic agents in glioma patients. BCNU and cisplatin are also being used to treat pediatric

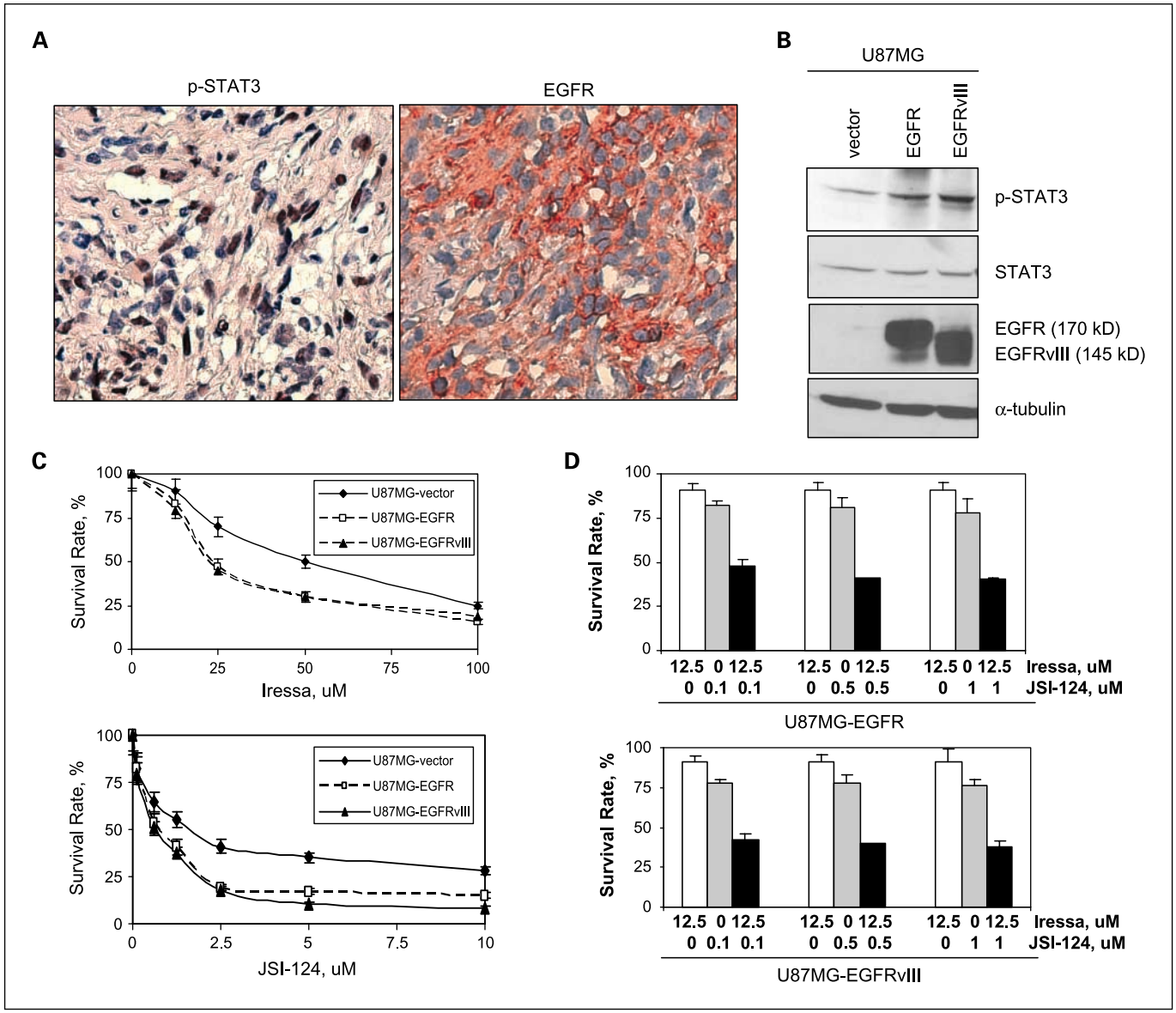

Fig. 5. Coexpression of EGFR with constitutively activated STAT3 was frequently detected in primary GBMs: JAK2/STAT3 inhibition sensitizes EGFR/EGFRvIII-expressing GBM cells to Iressa. *A,* we immunostained the cohort of human gliomas, which we previously analyzed for p-STAT3, for EGFR as we previously described (47). A representative GBM tumor containing both STAT3 constitutive activation (*left*) and EGFR (*right*) is shown. Adjacent tumor sections were used in these studies. *B,* stable U87MG-EGFR and U87MG-EGFRvIII cells expressed high levels of EGFR and EGFRvIII. All three stable cell lines were subjected to Western blot analyses for expression of EGFR, STAT3, and p-STAT3. Levels of α-tubulin were also determined as loading controls. Noticeably, U87MG-EGFR cell expressed wild-type EGFR (170 kDa), whereas U87MG-EGFRvIII cells expressed EGFRvIII with a lower molecular weight, 145 kDa. *C,* sensitivity of U87MG-EGFR and U87MG-EGFRvIII cells to Iressa and JSI-124. Both cell lines were treated with Iressa (0-100 μmol/L) or JSI-124 (0-10 μmol/L) for 48 h and survival rates were determined. Points, mean of three independent experiments; bars, SD. *D,* JSI-124 sensitized U87MG-EGFR and U87MG-EGFRvIII cells to Iressa treatments. Both cell lines were treated with Iressa (0 or 12.5 μmol/L), JSI-124 (0-1 μmol/L), or in combination for 48 h and survival rates were determined. Data were derived from three independent experiments.

Table 4. Sensitivity of medulloblastoma and malignant glioma cells to temozolomide, BCNU, and cisplatin

	Temozolomide	BCNU	Cisplatin
UW228	>200 μmol/L	>200 μmol/L	30 μmol/L
MGR1	>200 μmol/L	>200 μmol/L	9 μmol/L
MGR2	>100 μmol/L	95 μmol/L	40 μmol/L
MGR3	>200 μmol/L	190 μmol/L	82 μmol/L

NOTE: Tumor cells were treated with 0 to 200 μmol/L of temozolomide, BCNU, and cisplatin for 48 h and cell viability was determined. IC_{50} values are shown.

medulloblastomas, whereas temozolomide is under clinical evaluation for these patients. Unfortunately, the efficacy of these three agents in treating both medulloblastomas and malignant gliomas is only modest.

We found that human medulloblastoma UW228 and malignant glioma MGR1, MGR2, and MGR3 cell lines were highly resistant to temozolomide/TMZ and BCNU and modestly resistant to cisplatin/CDDP (Table 4). JSI-124 treatment significantly increased the sensitivity of UW228 and MGR3 cells to temozolomide (Fig. 6A) and BCNU (Fig. 6B), and in contrast, MGR1 and MGR2 cells were only modestly sensitive to the combination treatments. Importantly, JSI-124 strongly sensitized all cell lines, except for MGR2, to cisplatin and the effects were achieved by low doses of cisplatin (1-20 μmol/L; Fig. 6C). In light of the ability of JSI-124 to sensitize these tumor cells to low doses of cisplatin, we next examined whether the combination of cisplatin with JSI-124, at a molar ratio of 200:1, was synergistic in targeting medulloblastoma and malignant glioma cells. Median-effect analysis and CalcuSyn software were used to determine synergy, as previously described (9, 47). The results from these studies (Fig. 6D; Supplementary Fig. S6) show that combined uses of cisplatin and JSI-124 yielded significant synergistic cell kill in all four cell lines, as indicated by CI values <1.0. Taken together,

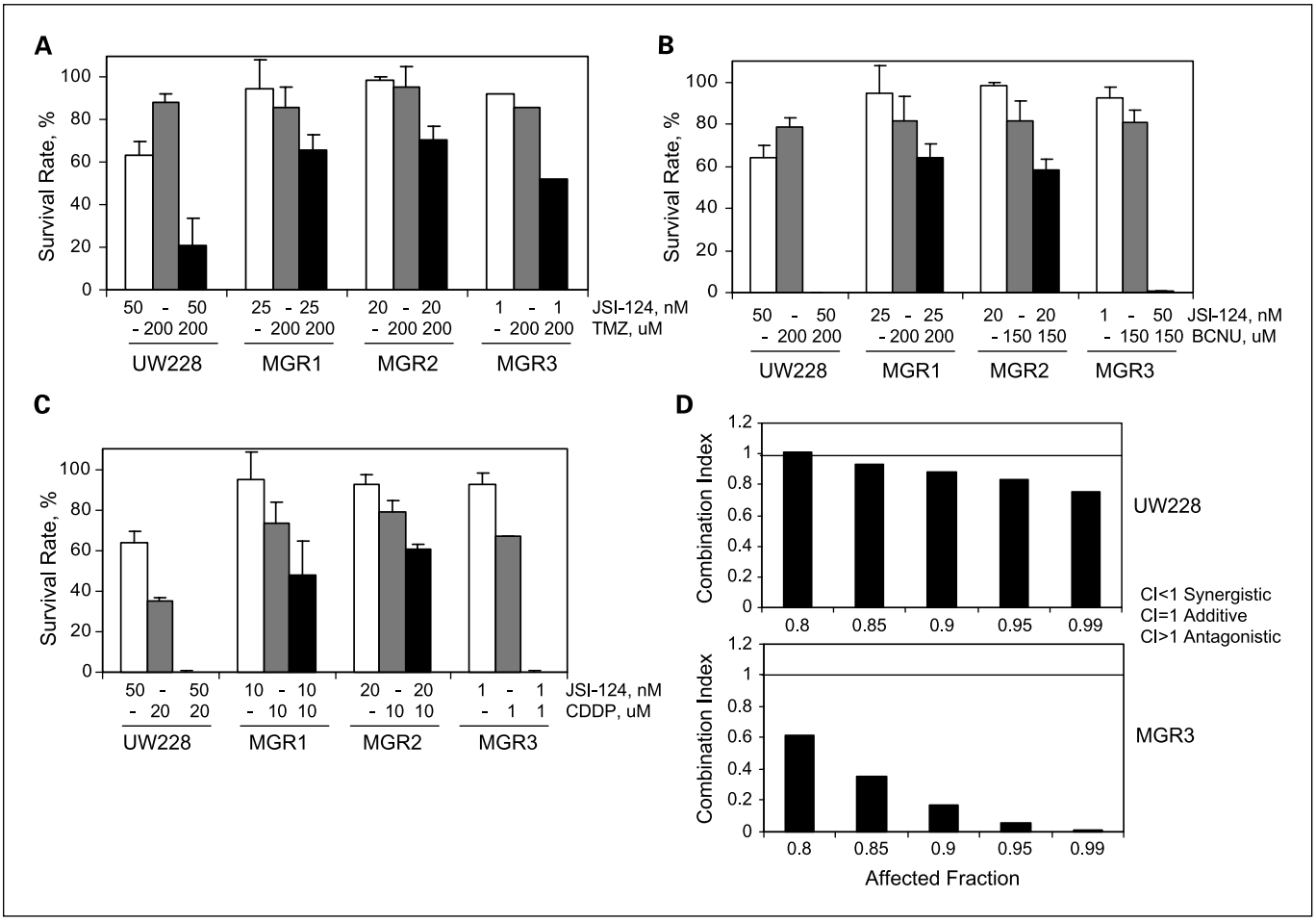

Fig. 6. STAT3/JAK2 inhibition by JSI-124 sensitized human malignant glioma and medulloblastoma cells to temozolomide, BCNU, and cisplatin and cooperated synergistically with cisplatin. The human malignant glioma MGR1, MGR2, and MGR3 and medulloblastoma UW228 cells were used in these studies. *A* to *C,* JSI-124 sensitized resistant medulloblastoma and glioma cells to temozolomide (*TMZ*), BCNU, and cisplatin (*CDDP*). Tumor cells were treated with single agents or JSI-124 in combination with temozolomide (*A*), BCNU (*B*), and cisplatin (*C*) for 48 h. Cell viability was then determined. Columns, mean of three independent experiments; bars, SD. *D,* cisplatin and JSI-124 targeted medulloblastoma and malignant glioma cells in a synergistic fashion. To determine whether a synergy existed between cisplatin and JSI-124, we did median-effect analysis to determine CI values, as previously described (9, 48). Combination of cisplatin with JSI-124 was mixed in the molar ratio of 200:1. UW228 and MGR3 cells were exposed to treatments for 48 h and cell viability was determined. CI ‹ 1: synergy, CI = 1: additive effect, CI › 1: antagonistic effect.

STAT3/JAK2 inhibition by JSI-124 sensitized human medulloblastoma and malignant glioma cells to temozolomide, BCNU, and cisplatin treatments and strongly cooperated with cisplatin resulting in synergistic cell death.

Discussion

We report in this study that the STAT3 pathway is highly deregulated in human medulloblastomas and gliomas, and a treatment target for sensitization to chemotherapy, and that STAT3 constitutive activation significantly coexists with EGFR in high-grade/malignant, but not low-grade, gliomas contributing to their resistance to anti-EGFR agents. Although STAT3 constitutive activation is frequently found in various human cancers, the extent of STAT3 constitutive activation in primary human gliomas, however, remains elusive. In this study, using p-STAT3 (Y705) as a measure of STAT3 activation, we found 40% (22 of 55) of grade I-IV primary gliomas to have constitutively active STAT3. This is consistent with other reports showing that approximately 50% to 60% of human breast tumors were found to contain constitutively activated STAT3 (10, 11). Moreover, we found that STAT3 was constitutively activated in 28.6% of low-grade (grades I and II) gliomas and 60% in high-grade (grades III and IV) gliomas. If only considering p-STAT3 negativity or positivity, we found the majority of the primary gliomas, 63.6% (35 of 55), to stain positively for p-STAT3, with 54.3% (19 of 35) in low-grade gliomas (grades I and II) and 80% (16/20) in high-grade gliomas (grade III and IV). In agreement with this finding, Schaefer et al. (26) previously reported 54.5% (6 of 11) and 81.8% (9 of 11), respectively, of low-grade and high-grade/malignant gliomas to contain p-STAT3. In contrast, another study observed p-STAT3 in <9% of high-grade gliomas (55). Those glioma cases that do not contain significant STAT3 activation are likely the result of either low STAT3 expression or the lack of aberrant upstream kinases that phosphorylate STAT3.

Despite that a high frequency of constitutively activated STAT3 was observed in human malignant gliomas, it remains undefined whether STAT3 constitutive activation is linked to the aggressiveness of these tumors. Here, we provide evidence, for the first time, that STAT3 constitutive activation is positively associated with glioma grade. This finding further suggests the potential pathologic significance of STAT3 activation in the aggressiveness of human gliomas.

In an attempt to profile the STAT3 pathway in human glioma cells, we found that tumor cells with hyperactive STAT3 tend to express high levels of cyclin D1 and VEGF and to activate the GAS and cyclin D1 promoters. To our best knowledge, this is the first study to investigate whether gliomas with activated STAT3 indeed express high cyclin D1 and VEGF, although overexpression of both genes in gliomas has been previously reported (56, 57). Our data also suggest that STAT3 suppression can lead to decreased expression of cyclin D1, a positive G_1 regulator, further implying that targeting STAT3 may inhibit glioma growth via reducing the expression of cyclin D1. In line with our observation that VEGF is expressed in human malignant glioma cells with hyperactive STAT3, tumor endothelial cells within highly vascularized gliomas have been reported to contain constitutively activated STAT3, which activates VEGFR-2 expression (26). This finding, together with our observation that malignant glioma cells frequently express high levels of VEGF, suggests that gliomas with activated STAT3 may have a VEGF/VEGFR autocrine loop to facilitate angiogenesis of malignant gliomas.

Targeting STAT3 as an anticancer strategy has emerged as a major area of research and several anti-STAT3 agents have been developed and evaluated in cultured cancer cells and in xenografts. For example, anti-STAT3 platinum compounds, CPA1 and CPA7, have shown antitumor activity in colon tumors (58). STA-21 targeted breast cancer cells (59). AG490 inhibited the growth of U251 GBM cells (60). WP1066, more potent than AG490, suppressed the growth of s.c. U87MG malignant gliomas (32). In addition to small-molecule inhibitors, STAT3 small interfering RNA has been shown to induce apoptosis in A172 GBM cells (53, 54). JSI-124 inhibited STAT3 phosphorylation leading to growth suppression of lung and breast tumors and cultured lymphoma cells and cervical and endometrial cancer cells (25, 30, 61, 62). The effect of JSI-124 in human gliomas was first tested in this study and the results showed a potent and significant inhibition of STAT3 activation and cell growth in human malignant glioma and medulloblastoma cells. To our best knowledge, JSI-124 displays the most potent killing effect thus far in cultured human glioma cells compared with other anti-STAT3 agents, such as AG490 and WP1066. We also showed for the first time that STAT3 inhibition led to medulloblastoma cell death.

JSI-124 was identified as a JAK2 inhibitor that suppresses STAT3 phosphorylation but displays much lower activities toward JAK1 and src (25). Although it is likely that JSI-124 may also inhibit STAT1 and STAT5 phosphorylation in addition to STAT3, the report by Nefedova et al. (61) indicated that JSI-124 has effects only on the phosphorylation of STAT3 but not on that of STAT1 or STAT5.

Also serve as an important anticancer target, EGFR and EGFRvIII are frequently overexpressed in human gliomas and associated with tumorigenesis (2, 63). Thus far, four anti-EGFR agents have been approved for cancer patients: gefitinib/Iressa for non–small cell lung cancer, monoclonal EGFR antibodies cetuximab and panitumumab for metastatic colorectal cancer, and erlotinib for metastatic non–small cell lung cancer. Their efficacy in treating glioma patients has been evaluated in clinical trials as single agent and in combination with other chemotherapeutic agents but with modest effects (2, 40, 41).

Mechanisms underlying the resistance to anti-EGFR therapy, however, remain unclear. The results in this study indicate that high STAT3 activity may contribute a novel mechanism underlying resistance of human GBMs to anti-EGFR therapy and that dual inhibition of both pathways potently and synergistically targets EGFR- and EGFRvIII-expressing human GBM cells. This is consistent with the observations from this study that EGFR frequently coexist with STAT3 constitutive activation in primary high-grade gliomas. In agreement with these observations, STAT3 has been shown to physically interact and functionally cooperate with EGFR, at both cytoplasmic and nuclear levels, to induce gene expression and regulate important cellular processes (9, 43). Activated cell-surface EGFR recruits and phosphorylates STAT3 at Y705, and in turn, p-STAT3 enters the nucleus to activate expression of several cancer-related genes. For example, EGFR cooperates with STAT3 to induce TWIST expression and facilitate epithelial-mesenchymal transition in cancers of the epithelial origin (11). On the other hand, nuclear EGFR interacts with STAT3 to activate expression of inducible nitric oxide synthase (9). Dual inhibition of EGFR and STAT3/

JAK2 led to synergistic killing of human breast and epidermoid carcinoma cells (9). Accumulatively, the results in this study solidify an important role that STAT3 constitutive activation plays in the resistance of EGFR/EGFRvIII-expressing high-grade gliomas to anti-EGFR therapy.

Current therapy for malignant gliomas and medulloblastomas, the most common brain tumors in adults and children, respectively, remains unsatisfactory and is in need of identification of novel targets and more effective, less toxic therapeutic strategies (1, 4). The results from this study provide new rationales for novel combinational therapies using anti-STAT3/JAK2 agents to sensitize EGFR/EGFRvIII-expressing malignant gliomas to anti-EGFR agents and to synergistically cooperate with the alkylating agent cisplatin in targeting both medulloblastoma and malignant glioma cells. These findings also prompt the need of a future evaluation of the therapeutic efficacy of STAT3-based combinational therapy in targeting high-grade/malignant gliomas and medulloblastomas.

Disclosure of Potential Conflicts of Interest

No potential conflicts of interest were disclosed.

References

1. Grossman SA, Batara JF. Current management of glioblastoma multiforme. Semin Oncol 2004;31:635–44.
2. Friedman HS, Bigner DD. Glioblastoma multiforme and the epidermal growth factor receptor. N Engl J Med 2005;353:1997–9.
3. Reardon DA, Rich JN, Friedman HS, Bigner DD. Recent advances in the treatment of malignant astrocytoma. J Clin Oncol 2006;24:1253–65.
4. Rood BR, MacDonald TJ, Packer RJ. Current treatment of medulloblastoma: recent advances and future challenges. Semin Oncol 2004;31:666–75.
5. Wechsler-Reya R, Scott MP. The developmental biology of brain tumors. Annu Rev Neurosci 2001;24:385–428.
6. Packer RJ, Sutton LN, Elterman R, et al. Outcome for children with medulloblastoma treated with radiation and cisplatin, CCNU, and vincristine chemotherapy. J Neurosurg 1994;81:690–8.
7. Darnell JE, Jr., Kerr IM, Stark GR. Jak-STAT pathways and transcriptional activation in response to IFNs and other extracellular signaling proteins. Science 1994;264:1415–21.
8. Fu XY. From PTK-STAT signaling to caspase expression and apoptosis induction. Cell Death Differ 1999;6:1201–8.
9. Lo H-W, Hsu S-C, Ali-Seyed M, et al. Nuclear interaction of EGFR and STAT3 in the activation of iNOS/NO pathway. Cancer Cell 2005;7:575–89.
10. Garcia R, Bowman TL, Niu G, et al. Constitutive activation of Stat3 by the Src and JAK tyrosine kinases participates in growth regulation of human breast carcinoma cells. Oncogene 2001;20:2499–513.
11. Lo H-W, Hsu S-C, Xia W, et al. Epidermal growth factor receptor cooperates with signal transducer and activator of transcription 3 to induce epithelial-mesenchymal transition in cancer cells via up-regulation of TWIST gene expression. Cancer Res 2007;67:9066–76.
12. Barre B, Avril S, Coqueret O. Opposite regulation of myc and p21waf1 transcription by STAT3 proteins. J Biol Chem 2003;278:2990–6.
13. Bowman T, Broome MA, Sinibaldi D, et al. Stat3-mediated Myc expression is required for Src transformation and PDGF-induced mitogenesis. Proc Natl Acad Sci U S A 2001;98:7319–24.
14. Yang E, Lerner L, Besser D, Darnell JE, Jr. Independent and cooperative activation of chromosomal c-fos promoter by STAT3. J Biol Chem 2003;278:15794–9.
15. Shirogane T, Fukada T, Muller JM, et al. Synergistic roles for Pim-1 and c-Myc in STAT3-mediated cell cycle progression and antiapoptosis. Immunity 1999;11:709–19.
16. Sinibaldi D, Wharton W, Turkson J, et al. Induction of p21WAF1/CIP1 and cyclin D1 expression by the Src oncoprotein in mouse fibroblasts: role of activated STAT3 signaling. Oncogene 2000;19:5419–27.
17. Karni R, Jove R, Levitzki A. Inhibition of pp60c-Src reduces Bcl-XL expression and reverses the transformed phenotype of cells overexpressing EGF and HER-2 receptors. Oncogene 1999;18:4654–62.
18. Niu G, Wright KL, Huang M, et al. Constitutive Stat3 activity up-regulates VEGF expression and tumor angiogenesis. Oncogene 2002;21:2000–8.
19. Wei D, Le X, Zheng L, et al. Stat3 activation regulates the expression of vascular endothelial growth factor and human pancreatic cancer angiogenesis and metastasis. Oncogene 2003;22:319–29.
20. Xie TX, Wei D, Liu M, et al. Stat3 activation regulates the expression of matrix metalloproteinase-2 and tumor invasion and metastasis. Oncogene 2004;23:3550–60.
21. Lowe C, Gillespie GA, Pike JW. Leukemia inhibitory factor as a mediator of JAK/STAT activation in murine osteoblasts. J Bone Miner Res 1995;10:1644–50.
22. Bromberg JF, Wrzeszczynska MH, Devgan G, et al. Stat3 as an oncogene. Cell 1999;98:295–303.
23. Huang S. Regulation of metastases by signal transducer and activator of transcription 3 signaling pathway: clinical implications. Clin Cancer Res 2007;13:1362–6.
24. Turkson J, Ryan D, Kim JS, et al. Phosphotyrosyl peptides block Stat3-mediated DNA binding activity, gene regulation, and cell transformation. J Biol Chem 2001;276:45443–55.
25. Blaskovich MA, Sun J, Cantor A, et al. Discovery of JSI-124 (cucurbitacin I), a selective Janus kinase/signal transducer and activator of transcription 3 signaling pathway inhibitor with potent antitumor activity against human and murine cancer cells in mice. Cancer Res 2003;63:1270–9.
26. Schaefer LK, Ren Z, Fuller GN, Schaefer TS. Constitutive activation of Stat3α in brain tumors: localization to tumor endothelial cells and activation by the endothelial tyrosine kinase receptor (VEGFR-2). Oncogene 2002;21:2058–65.
27. Rahaman SO, Vogelbaum MA, Haque SJ. Aberrant Stat3 signaling by interleukin-4 in malignant glioma cells: involvement of IL-13Rα2. Cancer Res 2005;65:2956–63.
28. Cattaneo E, Magrassi L, De-Fraja C, et al. Variations in the levels of the JAK/STAT and ShcA proteins in human brain tumors. Anticancer Res 1998;18:2381–7.
29. Yu H, Jove R. The STATs of cancer—new molecular targets come of age. Nat Rev Cancer 2004;4:97–105.
30. Chen CL, Hsieh FC, Lieblein JC, et al. Stat3 activation in human endometrial and cervical cancers. Br J Cancer 2007;96:591–9.
31. Turkson J, Jove R. STAT proteins: novel molecular targets for cancer drug discovery. Oncogene 2000;19:6613–26.
32. Iwamaru A, Szymanski S, Iwado E, et al. A novel inhibitor of the STAT3 pathway induces apoptosis in malignant glioma cells both *in vitro* and *in vivo*. Oncogene 2007;26:2435–44.
33. Wong AJ, Bigner SH, Bigner DD, et al. Increased expression of the epidermal growth factor receptor gene in malignant gliomas is invariably associated with gene amplification. Proc Natl Acad Sci U S A 1987;84:6899–903.
34. Sugawa N, Ekstrand AJ, James CD, Collins VP. Identical splicing of aberrant epidermal growth factor receptor transcripts from amplified rearranged genes in human glioblastomas. Proc Natl Acad Sci U S A 1990;87:8602–6.
35. Goumnerova LC. Growth factor receptors and medulloblastoma. J Neurooncol 1996;29:85–9.
36. Yamazaki H, Ohba Y, Tamaoki N, Shibuya M. A deletion mutation within the ligand binding domain is responsible for activation of epidermal growth factor receptor gene in human brain tumors. Jpn J Cancer Res 1990;81:773–9.
37. Ekstrand AJ, Sugawa N, James CD, Collins VP. Amplified and rearranged epidermal growth factor receptor genes in human glioblastomas reveal deletions of sequences encoding portions of the N- and/or C-terminal tails. Proc Natl Acad Sci U S A 1992;89:4309–13.
38. Wong AJ, Ruppert JM, Bigner SH, et al. Structural alterations of the epidermal growth factor receptor gene in human gliomas. Proc Natl Acad Sci U S A 1992;89:2965–9.
39. Nishikawa R, Ji XD, Harmon RC, et al. A mutant epidermal growth factor receptor common in human glioma confers enhanced tumorigenicity. Proc Natl Acad Sci U S A 1994;91:7727–31.
40. Omuro AMP, Faivre S, Raymond E. Lessons learned in the development of targeted therapy for malignant gliomas. Mol Cancer Ther 2007;6:1909–19.
41. Reardon DA, Quinn JA, Vredenburgh JJ, et al. Phase 1 trial of gefitinib plus sirolimus in adults with recurrent malignant glioma. Clin Cancer Res 2006;12:860–8.
42. Mellinghoff IK, Wang MY, Vivanco I, et al. Molecular determinants of the response of glioblastomas to EGFR kinase inhibitors. N Engl J Med 2005;353:2012–24.
43. Grandis JR, Drenning SD, Chakraborty A, et al. Requirement of Stat3 but not Stat1 activation for epidermal growth factor receptor-mediated cell growth *in vitro*. J Clin Invest 1998;102:1385–92.
44. Yamauchi T, Ueki K, Tobe K, et al. Tyrosine phosphorylation of the EGF receptor by the kinase Jak2 is induced by growth hormone. Nature 1997;390:91–6.
45. Ali-Osman F, Stein DE, Renwick A. Glutathione content and glutathione-*S*-transferase expression in 1,3-bis(2-chloroethyl)-1-nitrosourea-resistant human malignant astrocytoma cell lines. Cancer Res 1990;50:6976–80.
46. Lo H-W, Xia W, Wei Y, et al. Novel prognostic value of nuclear EGF receptor in breast cancer. Cancer Research 2005;65:338–48.
47. Chou TC, Talalay P. Quantitative analysis of dose-effect relationships: the combined effects of multiple drugs or enzyme inhibitors. Adv Enzyme Regul 1984;22:27–55.
48. Hsiao JR, Jin YT, Tsai ST, et al. Constitutive activation of STAT3 and STAT5 is present in the majority of nasopharyngeal carcinoma and correlates with better prognosis. Br J Cancer 2003;89:344–9.
49. Khoury JD, Medeiros LJ, Rassidakis GZ, et al. Differential expression and clinical significance of tyrosine-phosphorylated STAT3 in ALK$^+$ and ALK$^-$ anaplastic large cell lymphoma. Clin Cancer Res 2003;9:3692–9.
50. Nakamura JL. The epidermal growth factor receptor in malignant gliomas: pathogenesis and therapeutic implications. Expert Opin Ther Targets 2007;11:463–72.

51. Darnell JE, Jr. STATs and gene regulation. Science 1997;277:1630–5.
52. Schaefer LK, Menter DG, Schaefer TS. Activation of stat3 and stat1 DNA binding and transcriptional activity in human brain tumour cell lines by gp130 cytokines. Cell Signal 2000;12:143–51.
53. Konnikova L, Kotecki M, Kruger MM, Cochran BH. Knockdown of STAT3 expression by RNAi induces apoptosis in astrocytoma cells. BMC Cancer 2003;3:23.
54. Ren W, Duan Y, Yang Y, Ji Y, Chen F. Down-regulation of Stat3 induces apoptosis of human glioma cell: a potential method to treat brain cancer. Neurol Res 2008; 30:297–301.
55. Wang H, Wang H, Zhang W, et al. Analysis of the activation status of Akt, NFκB, and Stat3 in human diffuse gliomas. Lab Invest 2004;84:941–51.
56. Plate KH, Breier G, Weich HA, Risau W. Vascular endothelial growth factor is a potential tumour angiogenesis factor in human gliomas *in vivo*. Nature 1992;359:845–8.
57. Buschges R, Weber RG, Actor B, et al. Amplification and expression of cyclin D genes (CCND1, CCND2 and CCND3) in human malignant gliomas. Brain Pathol 1999;9:435–42; discussion 2–3.
58. Turkson J, Zhang S, Palmer J, et al. Inhibition of constitutive signal transducer and activator of transcription 3 activation by novel platinum complexes with potent antitumor activity. Mol Cancer Ther 2004;3:1533–42.
59. Song H, Wang R, Wang S, Lin J. A low-molecular-weight compound discovered through virtual database screening inhibits Stat3 function in breast cancer cells. Proc Natl Acad Sci U S A 2005;102:4700–5.
60. Rahaman SO, Harbor PC, Chernova O, et al. Inhibition of constitutively active Stat3 suppresses proliferation and induces apoptosis in glioblastoma multiforme cells. Oncogene 2002;21:8404–13.
61. Nefedova Y, Nagaraj S, Rosenbauer A, et al. Regulation of dendritic cell differentiation and antitumor immune response in cancer by pharmacologic-selective inhibition of the janus-activated kinase 2/signal transducers and activators of transcription 3 pathway. Cancer Res 2005;65: 9525–35.
62. Shi X, Franko B, Frantz C, Amin HM, Lai R. JSI-124 (cucurbitacin I) inhibits Janus kinase-3/signal transducer and activator of transcription-3 signalling, downregulates nucleophosmin-anaplastic lymphoma kinase (ALK), and induces apoptosis in ALK-positive anaplastic large cell lymphoma cells. Br J Haematol 2006;135:26–32.
63. Bigner SH, Humphrey PA, Wong AJ, et al. Characterization of the epidermal growth factor receptor in human glioma cell lines and xenografts. Cancer Res 1990;50:8017–22.